Cold heavy oil reservoir characterization: wormhole modeling and seismic responses

Xiaoqin Cui*, Laurence R. Lines and Edward S. Krebes
xicui@ucalgary.ca

Summary

Wormholes form fractural networks leading to increased reservoir permeability in the cold heavy oil production with sand (CHOPS). We extend a generalized homogeneous approach to present an algorithm of the finite difference scheme with the fracture parameters, modeling the wormholes of CHOPS and the recorded synthetic seismograms from wormholes based on the non-welded contact theory (Schoenberg, 1980). The PP and PS seismic characters, such as amplitude, frequency, and travel time (velocity) will vary with the fractural network wormhole features. 4D seismic time-lapse technology can be used to monitor CHOPS production and avoid invalid drilling.

3D finite difference scheme for wormholes modeling

During the cold production process, sand, oil, water, and gas are produced simultaneously by using progressive cavity pumps which generate high-porosity fractal network (channels) termed "wormholes" (Lines et al., 2008). The pattern of the grow wormholes looks like the fractal root system of a plant that has random direction of the fractures in the pay zone (Yuan et al., 1999).

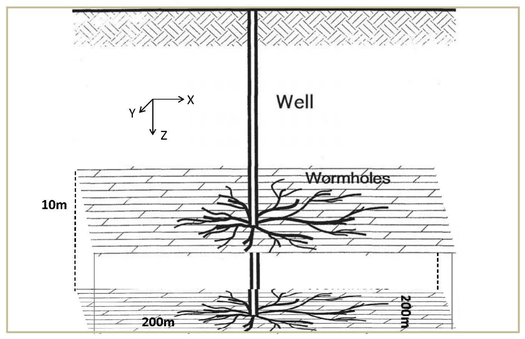

FIG. 1. A schematic of a 3D wormhole model (Modified Miller et al, 1999)

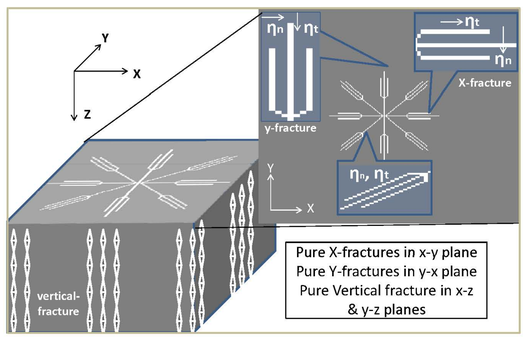

FIG. 2. A numerical model of a 3D wormhole.

FD scheme of the wormhole based on the extended generalized homogeneous approach with the non-welded contact slip interface theory.

$$\varphi^{t+\Delta t}_{x,y,z} = 2\varphi^{t}_{x,y,z} - \varphi^{t-\Delta t}_{x,y,z} + \frac{1}{\rho}\left(\frac{\Delta t}{h}\right)^2 \{A_f(\varphi^{t}_{x+\Delta x,y,z} - 2\varphi^{t}_{x,y,z} + \varphi^{t}_{x-\Delta x,y,z}) +$$

$$B_f(\varphi^{t}_{x,y+\Delta y,z} - 2\varphi^{t}_{x,y,z} + \varphi^{t}_{x,y-\Delta y,z}) + C_f(\varphi^{t}_{x,y,z+\Delta z} - 2\varphi^{t}_{x,y,z} + \varphi^{t}_{x,y,z-\Delta z}) +$$

$$\frac{1}{4}D_f(\varphi^{t}_{x+\Delta x,y+\Delta y,z} - \varphi^{t}_{x+\Delta x,y-\Delta y,z} - \varphi^{t}_{x-\Delta x,y+\Delta y,z} + \varphi^{t}_{x-\Delta x,y-\Delta y,z}) +$$

$$\frac{1}{4}E_f(\varphi^{t}_{x+\Delta x,y,z+\Delta z} - \varphi^{t}_{x+\Delta x,y,z-\Delta z} - \varphi^{t}_{x-\Delta x,y,z+\Delta z} + \varphi^{t}_{x-\Delta x,y,z-\Delta z}) +$$

$$\frac{1}{4}F_f(\varphi^{t}_{x,y+\Delta y,z+\Delta z} - \varphi^{t}_{x,y+\Delta y,z-\Delta z} - \varphi^{t}_{x,y-\Delta y,z+\Delta z} + \varphi^{t}_{x,y-\Delta y,z-\Delta z})\}$$

$$A_f = \begin{bmatrix} \frac{\lambda+2\mu}{1+\varphi} & 0 & 0 \\ 0 & \frac{\mu}{1+\varepsilon_y^y} + \frac{\mu}{1+\varepsilon_y^x} & 0 \\ 0 & 0 & \frac{\mu}{1+\varepsilon_y^y} + \frac{\mu}{1+\varepsilon_x^x} \end{bmatrix}, \quad B_f = \begin{bmatrix} \frac{\mu}{1+\varepsilon_x^y} + \frac{\mu}{1+\varepsilon_x^x} & 0 & 0 \\ 0 & \frac{\lambda+2\mu}{1+\varphi} & 0 \\ 0 & 0 & \frac{\mu}{1+\varepsilon_y^y} + \frac{\mu}{1+\varepsilon_x^x} \end{bmatrix}, \quad E_f = \begin{bmatrix} 0 & 0 & \frac{\lambda}{1+\varphi} + \frac{\mu}{1+\varepsilon_x^y} + \frac{\mu}{1+\varepsilon_x^x} \\ 0 & 0 & 0 \\ \frac{\lambda}{1+\varphi} + \frac{\mu}{1+\varepsilon_Y^y} + \frac{\mu}{1+\varepsilon_x^x} & 0 & 0 \end{bmatrix}$$

$$C_f = \begin{bmatrix} \frac{\mu}{1+\varepsilon_x^y} + \frac{\mu}{1+\varepsilon_x^x} & 0 & 0 \\ 0 & \frac{\mu}{1+\varepsilon_y^y} + \frac{\mu}{1+\varepsilon_y^x} & 0 \\ 0 & 0 & \frac{\lambda+2\mu}{1+\varphi} \end{bmatrix}, \quad D_f = \begin{bmatrix} 0 & \frac{\mu}{1+\varepsilon_x^y} + \frac{\mu}{1+\varepsilon_x^x} & 0 \\ \frac{\mu}{1+\varepsilon_Y^y} + \frac{\mu}{1+\varepsilon_Y^x} & 0 & 0 \\ 0 & 0 & 0 \end{bmatrix}, \quad F_f = \begin{bmatrix} 0 & 0 & 0 \\ 0 & 0 & \frac{\lambda}{1+\varphi} + \frac{\mu}{1+\varepsilon_Y^y} + \frac{\mu}{1+\varepsilon_Y^x} \\ 0 & \frac{\mu}{1+\varepsilon_Y^y} + \frac{\mu}{1+\varepsilon_x^x} & 0 \end{bmatrix}$$

λ and μ are medium parameters. Ø and ε are the dimensionless non-weldedness parameters that relate to fracture compliance parameters (Slawinski, 1999).

Synthetic seismograms

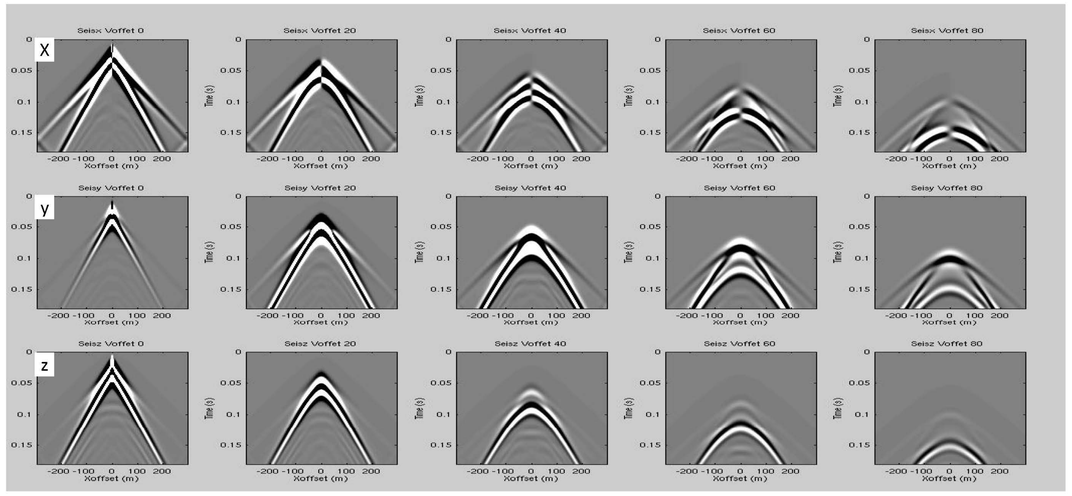

FIG. 3 Three components synthetic seismograms

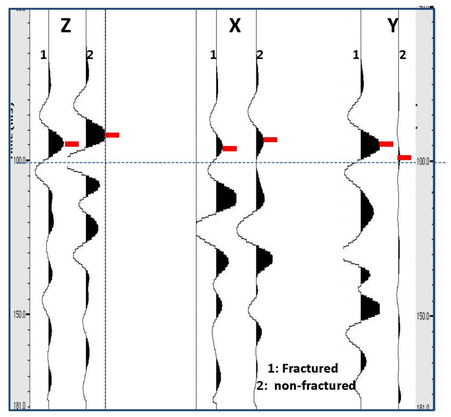

FIG. 4 The direction of the fracture effects the velocity

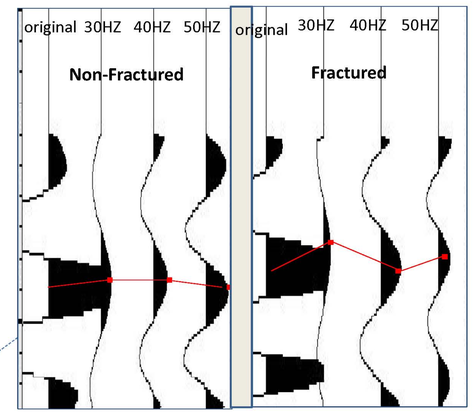

FIG. 5 The fracture causing the frequency dispersion

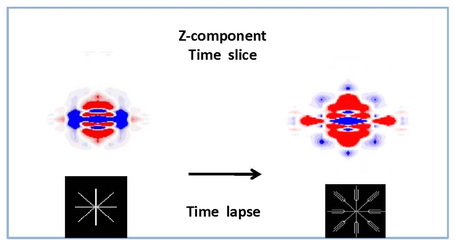

FIG. 6 z-component time slices of 4D time lapse data

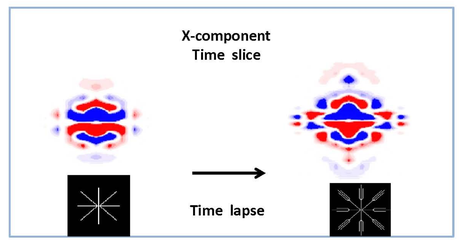

FIG. 7 x-component time slices of 4D time lapse data

Conclusions

A generalized homogeneous approach of finite difference method is extended for the 3D Seismic modeling of wormhole feature. Synthetic seismic data can be affected by wormholes demonstrating azimuthal anisotropy and frequency dispersion. Time-lapse data time slice is method to detect wormhole growth, which is used to evaluate reservoir permeability for enhancing oil & gas recovery and to avoid invalid drilling.